AIP | Applied Physics Letters

Metal cluster's effect on the optical properties of cesium bromide thin films

Kuldeep Kumar, P. Arun, Chhaya Ravi Kant, and Bala Krishna Juluri

Citation: Appl. Phys. Lett. **100**, 243106 (2012); doi: 10.1063/1.4729061
View online: http://dx.doi.org/10.1063/1.4729061
View Table of Contents: http://apl.aip.org/resource/1/APPLAB/v100/i24
Published by the American Institute of Physics.

Metal cluster's effect on the optical properties of cesium bromide thin films

Kuldeep Kumar,[1] P. Arun,[1,a)] Chhaya Ravi Kant,[2] and Bala Krishna Juluri[3,b)]
[1]*Material Science Research Lab, S.G.T.B. Khalsa College, University of Delhi, Delhi 110 007, India*
[2]*Department of Applied Sciences, Indira Gandhi Institute of Technology, Guru Gobind Singh Indraprastha University, Delhi 110 006, India*
[3]*Pacific Integrated Energy Inc., San Diego, California 92130, USA*

(Received 13 February 2012; accepted 14 May 2012; published online 13 June 2012)

Cesium bromide (CsBr) films grown on glass substrates by thermal evaporation showed prominent absorption peaks in the UV-visible region. Interestingly, these absorption spectra showed peaks which red shifted over time in ambient exposure. Structural and morphological studies suggested decrease in particle size overtime which was unusual. Electron micrographs show the formation of "daughter" cesium nanorods from parent CsBr particles. Theoretical calculations show the optical behavior observed to be due to localized surface plasmon resonance resulting from cesium nanorods. © *2012 American Institute of Physics*. [http://dx.doi.org/10.1063/1.4729061]

Alkali halides (AH) have been extensively studied in the 1960's to understand the variation in energy band structure with changing lattice constant.[1] Their simple crystal structures, experimentally determinable phase transitions, and reproducible variation in properties due to pressure made them popular research candidates.[2] AH are considered excellent photon-absorbing materials in the x-ray and ultraviolet regions where usage results in formation of color-centers.[3–6] In addition, AH's have gained popularity in detector and optoelectronics applications due to their excellent quantum efficiency.[7] However, practical application of AH films suffered due to their high reactivity with atmospheric water vapor[8] making them difficult to maintain. Cesium bromide (CsBr), which exhibits a relatively higher stability when exposed to air,[9] was therefore of interest. For example, CsBr films deposited on thin metal layers have been used as an electron source[10] and as a protective layer of a photocathode.[11]

During our previous studies on CsI (Ref. 12) thin films, we observed optical absorption peaks in the visible regime. Similarly, we have noticed absorption peaks in CsBr (present work) thin films. We believe that these absorption peaks reflect plasmon resonances associated with Cs metal clusters that have been formed from CsBr parent nanoparticles. These observations are in inline with the idea put forward by Emel'yanov *et al*. and others.[13,14] They claimed that the various defect states (such as F-centers) present in AH, when provided with the right conditions lead to the formation of alkali metal clusters. In this report, we study optical absorption by CsBr thin films, the formation of cesium nanorods in CsBr thin films due to aging effect and their effect on the optical properties of CsBr thin films. The work not only discusses ageing in samples which is of importance to users of AH devices but also shows formation of surface plasmon resonances (SPRs) in AH films with potential use as sensors.

Cesium bromide thin films of various thickness were deposited by thermal evaporation on microscopy glass substrates at room temperature and at a pressure of 1.4×10^{-5} Torr using 99.98% pure CsBr powder. Optical properties of these thin films were first studied by measuring extinction spectra. Spectra were taken at various time intervals for two sets of samples: those that were placed in a desiccator and others exposed to air. Optical absorption spectra for samples of 840 nm thickness kept in air are shown in Figure 1(a). A strong extinction peak at ~500 nm was observed in spectra obtained just after the deposition of thin films. Studies on CsI thin films revealed similar peaks in their UV-visible absorption spectra in our earlier studies.[12] However, the peak position red-shifted with time and the extinction intensity decreased with time. The shift in peak position showed a linear trend with time and the rate of change was found to be dependent on film thickness. Thicker film samples showed more red shift than thin film samples (Figure 1(b)). However, the optical spectra of samples preserved in desiccator revealed significantly less red shift of peak position and peak intensity with time indicating this effect to be a function of ambient atmosphere. This led us to believe that the peak position in extinction spectra could be due to the formation of Cs nanoparticles in CsBr thin films and excitation of localized surface plasmon resonances (LSPRs) in these nanoparticles. Plasmon resonances are excited due to the interaction of electromagnetic fields with free electrons in metal nanoparticles whose size is smaller or comparable to that of wavelength of incident light.[15] Both the LSPR's peak position and its intensity are strongly dependent on the metal cluster's size, shape, and the refractive index of the surrounding media. These results, hence, indicate some systematic and continuous structural and compositional changes in the film over time.

To understand the effect of exposure time on the absorption spectra of CsBr films, we performed structural and compositional studies. Structural information was obtained by field-emission scanning electron microscopy (FESEM) and transmission electron microscopy (TEM). Composition studies were obtained by energy dispersive x-ray spectroscopy (EDX), selected area electron diffraction (SAED), and x-ray diffraction. Figure 2(a) shows a representative FESEM image of a CsBr thin film. It can be seen that these films consist of random and uniformly spaced nanoparticles with an

a)Electronic mail: arunp92@physics.du.ac.in.
b)Electronic mail: bkj@pienergy.com.

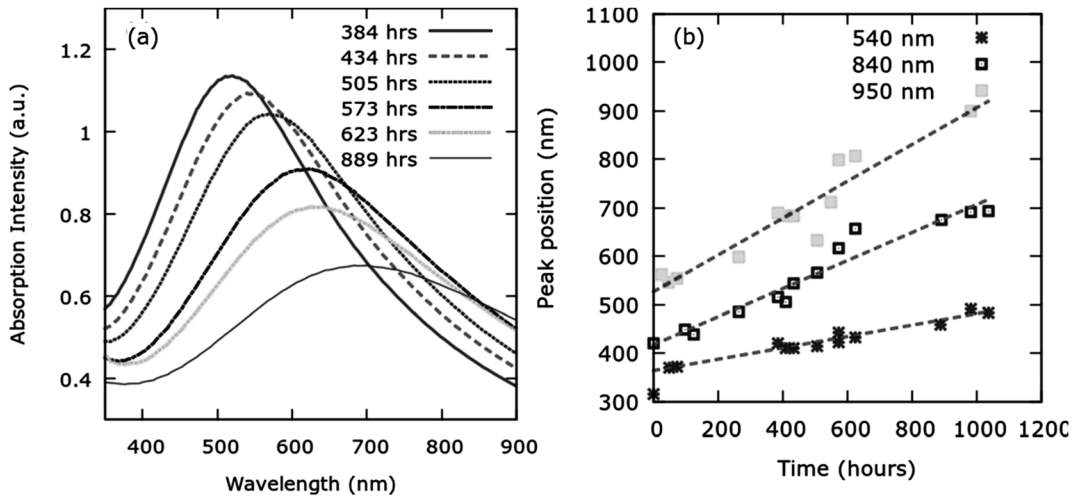

FIG. 1. (a) Absorbance spectra of CsBr thin film taken at different time intervals and (b) peak absorption wavelength of different CsBr films thickness as a function of time.

average particle size of $\sim 1\ \mu$m. A close-up (outlined circles in Figure 2(a)) shows interconnected bridges at their edges. These structures increase in length as the particles move apart. As the nanoparticles moves apart, the cylindrical shaped bridge is retained by one of the particles. Some of these bridges finally break off as "child" nanorods and fall into the background leaving behind a smooth spherical nanoparticle. Size statistics done on the freshly deposited thin film samples kept in dessicator and those exposed in air for 1100 h revealed a difference in average particle size (from 1 μm to 0.95 μm). The particle density of samples kept in air ($0.91\ \mu m^{-2}$) was found to be nearly twice that of the counterpart kept in the desiccator ($0.52\ \mu m^{-2}$). The full width at half maxima (FWHM) of the Gaussian fit to the histograms also reflect a narrower distribution for the samples maintained in the desiccator. These results suggest nanoparticles of the film split giving rise to smaller nanoparticles. Also, this process of nanoparticle breaking is encouraged in samples kept in air. EDX of "child" nanorods and parent nanoparticles show that they are primarily made up of cesium. These results indicate displacement of Cs metal from CsBr nanoparticle to the surface of parent nanoparticle and formation of Cs child nanorods. This would mean that CsBr parent nanoparticles should have a displaced Cs layer on the surface to form an "insulator-metal" or a "core-shell" structure. This was also confirmed by TEM micro-graphs, which clearly showed distinct regions of core and shell (Figure 2(b)). In addition, SAED taken on one of the core of the parent nanoparticle reveal characteristic spots indicating the crystalline nature of the "core" (see Figure 3). The major spots of the SAED are arranged on two distinct rings corresponding to the (110) and (211) peaks of CsBr as indexed in ASTM Card No. 73-0391. Similar analysis of the child nanorod shows their crystallinity with three distinct ring corresponding to the (200), (331), and (220) planes of cesium as given in the ASTM Card No 18-0325.

To understand the breaking of child nanorods from parent nanoparticles, x-ray diffraction was performed to estimate stresses in the nanoparticles and estimate mass variation with time. X-ray diffraction of the samples soon after deposition reveal two major peaks at $2\theta \approx 29.3^\circ$ and $\approx 52^\circ$. Both CsBr and Cs have peaks in and around these position as given in ASTM Card (Ref. 16) Nos. 73-0391 and 18-0325, respectively. Peaks of CsBr and Cs are just resolvable and Lorentzian peaks can be inserted at peak positions given by the ASTM cards. Figure 3 compares x-ray diffraction spectra of freshly prepared CsBr and samples after 794 h. The relative increase in the Cs peak intensity at

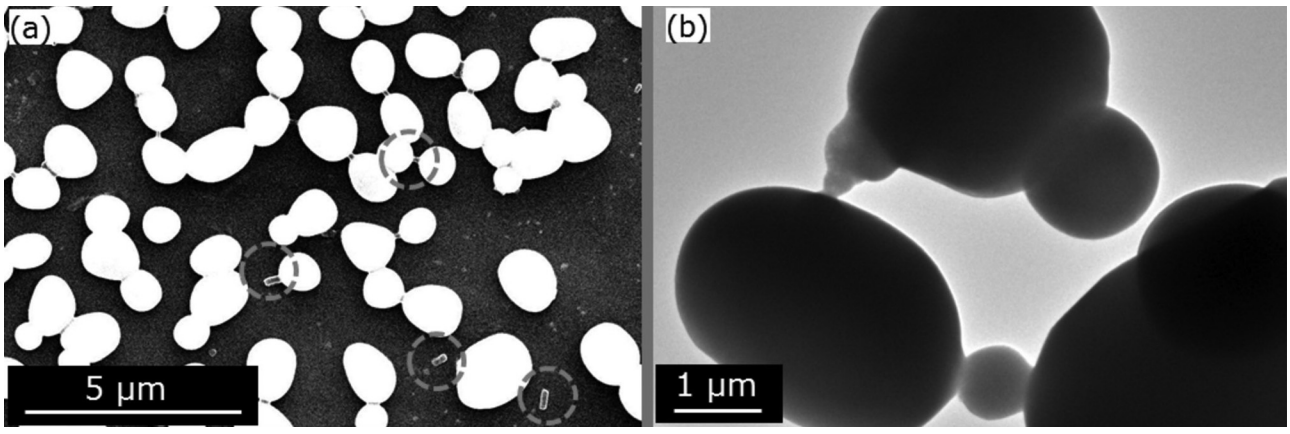

FIG. 2. (a) SEM image of CsBr thin films, green circles show the presence of bridges that fall of to form daughter cesium nanorods and (b) a TEM image showing a close-up view of bridges.

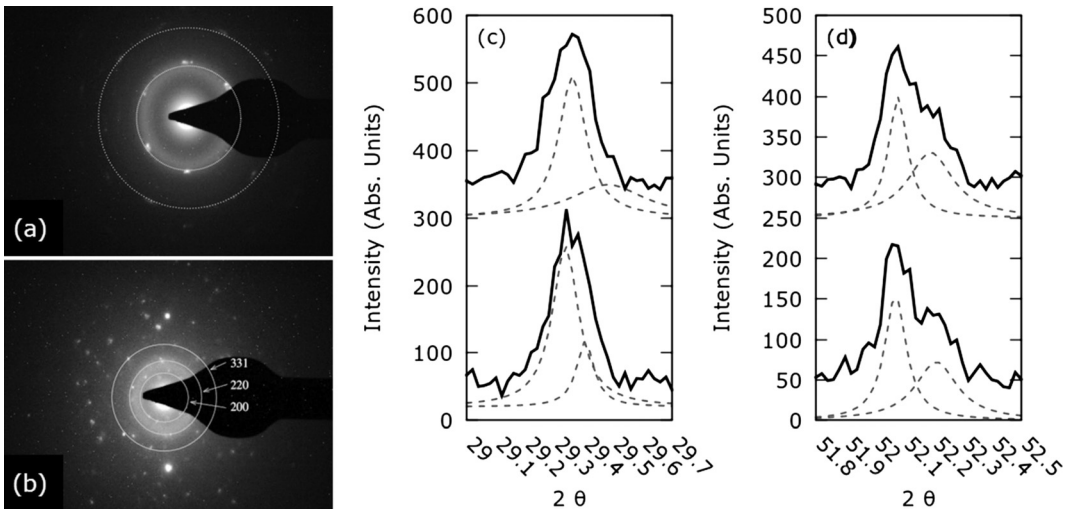

FIG. 3. SAED of (a) core and (b) shell/nanorod confirm the formation of CsBr core along with Cs shell and nanorods. Formation of core-shell with nanorods structures is also confirmed by the deconvolutable XRD peaks. Two prominent XRD peaks at (a) ∼29° and (b) ∼52° are shown.

$2\theta \approx 52^\circ$ with time indicates the formation of Cs in CsBr films with time. The sizes (Table I) of CsBr core in parent nanoparticles and Cs child nanorods were calculated from the x-ray diffraction peak's FWHM using Scherrer formula (see Figure 3).[17] Size of parent CsBr nanoparticle and child Cs nanorod were found to decrease with increasing time. The size of CsBr parent nanoparticles according to x-ray diffraction is smaller than the sizes observed in TEM. This indicates that the boundaries of the core, as viewed in the TEM micrographs, enclose crystalline region along with amorphous CsBr. More importantly, the CsBr peaks were found to have shifted to the right as compared to the peak positions given in the ASTM Card. This would indicate that the CsBr lattice is in a state of stress with compressive forces acting on it. The stress in the film was calculated after evaluating the strain using the relation $\frac{\Delta d}{d} = \frac{d_{obs} - d_{ASTM}}{d_{obs}}$, where d_{obs} is the experimentally observed d-spacing and d_{ASTM} is the corresponding peak's d-spacing as reported in the ASTM card.[18] The stress is then determined by multiplying the strain by the elastic constant of the material. The calculated strain on the (110) plane of CsBr changed from −0.0023 to −0.0028 with an elapse of 900 h. We believe it is this stress that contributes to the required energy for bromide's disassociation.

As revealed in the SEM and TEM images, CsBr thin films consist of pure CsBr nanoparticles, CsBr shell particles (CsBr core and Cs shell) and Cs nanorods. To understand the experimentally observed optical properties of CsBr thin films and the effect of time on the absorption peak position, we calculated the extinction spectra of these structures using theoretical methods. Extinction of the former two particle types were solved by Mie scattering formulation, but these particle types did not show absorption/extinctions peaks in the visible regime. Approximating Cs nanorods as prolate spheroids, extinction spectra were calculated using Gans theory.[19] The dielectric function of Cs metal was obtained from Smith *et al.*[20,21] The Cs nanorods were assumed to be surrounded by vacuum. Different geometries of prolate spheroids were considered and extinction spectra were calculated using Gans theory. Figure 4 shows the extinction spectra of particles with the minor radius of the prolate spheroid fixed at 100 nm and the major radius varied from 1000 to 200 nm (aspect ratio varied from 10 to 2 and effective particles size varied from 215 to 125 nm). One can observe that all the shapes and sizes of spheroids exhibit extinction peaks in the visible regime and near infrared. The peaks in the visible regime represent the transverse modes and the peaks in the near infrared represent the longitudinal modes. The transverse peak positions red-shifted with decrease in aspect ratio and the intensity of the extinction spectra decreased with reduced particle size. These results can be qualitatively

TABLE I. Particle size of CsBr and Cs as calculated from the x-ray diffraction pattern.

Time (h)	CsBr size (nm)	Cs size (nm)
22	65 ± 6	88 ± 8
112	55 ± 4	76 ± 8
794	58 ± 6	55 ± 6
1034	34 ± 3	…

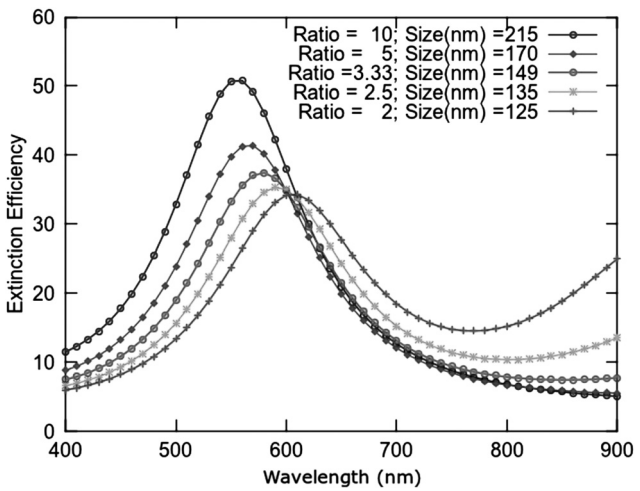

FIG. 4. Absorption spectra of Cs nano-rods calculated using Gans model. Family of curves show a redshift with average grain size and decreasing aspect ratio.

compared with experimental results (Figure 1) and indicate that the optical absorption peaks seen in experiments can be correlated to the transverse plasmon modes excited in Cs nanorods. In addition, the trend of red shift of absorption peaks and decrease in the absorption peak intensity observed in calculations matches qualitatively with the trend observed in experiments. These results support the hypothesis that with time, the Cs nanorods decrease in aspect ratio and size, resulting in redshifting of absorption peaks and decreased peak intensities.

Experimental data suggests that the stress in the as-grown films lead to the formation of defects caused by the bromide atom's displacement. These defects start collecting together to form clusters. With the curvature of the particle's surfaces contributing the maximum stress, the formation of cesium at the particle surfaces can be understood. This surface cesium around cesium bromide not only contributes to the core-shell structures present in the film but are also a site for formation of cesium nanorods. With time, the shell-core particle size decreases along with decrease in the average particle size of the cylindrical rods. Comparing the results with theoretical simulations suggest cylindrical particles contribute to SPR peaks in the visible wavelengths with decreasing particle size accompanied with increasing aspect ratio (ratio of diameter to length) leading to a red-shift in the peak position. These observations are of interest and may be exploited for applications in sensors or detectors. The fact that the rate at which the SPR peak moves to higher wavelengths depends on nature of ambient atmosphere suggests these can be used to measure humidity.

The authors would like to express their sincere gratitude to Department of Science and Technology (DST) India for the financial assistance (SR/NM.NS-28/2010) given for carrying out this work. The authors thank Justin Hallas for helpful discussions.

[1]H. Fujita, K. Yamauchi, A. Akasaka, H. Irie, and S. Masunaga, J. Phys. Soc. Jpn. **68**, 1994 (1999).
[2]M. B. Nardelli, S. Baroni, and P. Giannozzi, Phys. Rev. B **51**, 8060 (1995).
[3]P. V. Mitchell, D. A. Wiegand, and R. Simoluchowski, Phys. Rev. **121**, 484 (1961).
[4]F. T. Goldstein, Phys. Status Solidi B **20**, 379 (1967).
[5]M. Elango, C. Gahwiller, and F. C. Brown, Solid State Commun. **8**, 893 (1970).
[6]B. R. Sever, N. Kristianpollar, and F. C. Brown, Phys. Rev. B **34**, 1257 (1986).
[7]J. I. Larruquert, J. A. Mendez, J. A. Aznarez, A. S. Tremsin, and O. H. W. Siegmund, Appl. Opt. **41**, 2532 (2002).
[8]G. Yoshikawa, M. Kiguchi, K. Ueno, and A. Saiki, Surf. Sci. **554**, 220 (2003).
[9]*CRC Handbook of Chemistry and Physics*, edited by W. M. Haynes (CRC, USA, 2011).
[10]J. R. Maldonato, Z. Liu, D. H. Dowell, R. E. Kirby, Y. Sun, P. Pianetta, and F. Pease, Microelectron. Eng. **86**, 529 (2009).
[11]A. Buzulutskov, E. Shafer, A. Breskin, R. Chechik, and M. Prager, Nucl. Instrum. Methods A **400**, 173 (1997).
[12]K. Kumar, P. Arun, C. R. Kant, N. C. Mehra, and V. Methew, Appl. Phys. A **99**, 305 (2010).
[13]V. I. Emel'yanov, Laser Phys. **2**, 389 (1992).
[14]S. Seaglione, R. M. Montereali, V. Mussi, and E. Nichelatti, J. Optoelectron. Adv. Mater. **7**, 207 (2005).
[15]U. Kreibig and M. Vollmer, *Optical Properties of Metal Clusters* (Springer, Berlin, 1995).
[16]American Society for Testing Material (ASTM) cards is now compiled under the name "Powder Diffraction File (PDF).
[17]B. D. Cullity, *Elements of X-ray Diffraction*, 2nd ed. (Addisson-Wesley, NY, 1978).
[18]A. L. Patterson, Phys. Rev. **56**, 978 (1939).
[19]R. Gans, Ann. Phys. **47**, 270 (1915).
[20]N. V. Smith, Phys. Rev. B **2**, 2840 (1970).
[21]H. Chen, L. Shao, K. C. Woo, T. Ming, H. Lin, and J. Wang, J. Phys. Chem. C **113**, 17691 (2009).